Journal of Molecular and Cellular Cardiology 57 (2013) 13–22

Contents lists available at SciVerse ScienceDirect

Journal of Molecular and Cellular Cardiology

journal homepage: www.elsevier.com/locate/yjmcc

Original article

Familial hypertrophic cardiomyopathy: Functional effects of myosin mutation R723G in cardiomyocytes

Theresia Kraft [a,*], E. Rosalie Witjas-Paalberends [b], Nicky M. Boontje [b], Snigdha Tripathi [a], Almuth Brandis [c], Judith Montag [a], Julie L. Hodgkinson [a], Antonio Francino [d], Francisco Navarro-Lopez [d], Bernhard Brenner [a], Ger J.M. Stienen [b], Jolanda van der Velden [b]

[a] Molecular and Cell Physiology, Hannover Medical School, D-30625 Hannover, Germany
[b] Laboratory for Physiology, Institute for Cardiovascular Research, VU University Medical Center, Amsterdam, The Netherlands
[c] Institute for Pathology, Hannover Medical School, D-30625 Hannover, Germany
[d] Hospital Clinic/IDIBAPS, University of Barcelona, 08036 Barcelona, Spain

ARTICLE INFO

Article history:
Received 10 December 2012
Accepted 3 January 2013
Available online 11 January 2013

Keywords:
Familial hypertrophic cardiomyopathy
β-Myosin missense mutation R723G
Cardiomyocyte function
Slow skeletal muscle
Myofibrillar disarray
Calcium-sensitivity

ABSTRACT

Familial Hypertrophic Cardiomyopathy (FHC) is frequently caused by mutations in the β-cardiac myosin heavy chain (β-MyHC). To identify changes in sarcomeric function triggered by such mutations, distinguishing mutation effects from other functional alterations of the myocardium is essential. We previously identified a direct effect of mutation R723G ($MyHC_{723}$) on myosin function in slow *Musculus soleus* fibers. Here we investigate contractile features of left ventricular cardiomyocytes of FHC-patients with the same $MyHC_{723}$-mutation and compare these to the *soleus* data.

In mechanically isolated, triton-permeabilized $MyHC_{723}$-cardiomyocytes, maximum force was significantly lower but calcium-sensitivity was unchanged compared to donor. Conversely, $MyHC_{723}$-*soleus* fibers showed significantly higher maximum force and reduced calcium-sensitivity compared to controls. Protein phosphorylation, a potential myocardium specific modifying mechanism, might account for differences compared to *soleus* fibers. Analysis revealed reduced phosphorylation of troponin I and T, myosin-binding-protein C, and myosin-light-chain 2 in $MyHC_{723}$-myocardium compared to donor. Saturation of protein-kinaseA phospho-sites led to comparable, i.e., reduced $MyHC_{723}$-calcium-sensitivity in cardiomyocytes as in *M. soleus* fibers, while maximum force remained reduced. Myofibrillar disarray and lower density of myofibrils, however, largely account for reduced maximum force in $MyHC_{723}$-cardiomyocytes.

The changes seen when phosphorylation of sarcomeric proteins in myocardium of affected patients is matched to control tissue suggest that the R723G mutation causes reduced Ca^{++}-sensitivity in both cardiomyocytes and *M. soleus* fibers. In $MyHC_{723}$-myocardium, however, hypophosphorylation can compensate for the reduced calcium-sensitivity, while maximum force generation, lowered by myofibrillar deficiency and disarray, remains impaired, and may only be compensated by hypertrophy.

1. Introduction

Familial Hypertrophic Cardiomyopathy (FHC) is the most frequent genetically transmitted cardiac disease with a prevalence of 1:500 [1]. It is often characterized by asymmetric hypertrophy of left ventricular (LV) wall and septum and by an increased risk for sudden cardiac death particularly in young adults [2]. Myocyte disarray and interstitial fibrosis are hallmarks of FHC. Nearly all genotyped FHC cases revealed mutations in sarcomeric proteins. Yet, the underlying functional changes at the cardiomyocyte level possibly initiating disease development are still largely unknown.

To investigate mechanisms triggering FHC pathogenesis we focused on mutations in the β-cardiac myosin heavy chain (β-MyHC) gene (*MYH7*). *MYH7* mutations are responsible for approximately 30–40% of all genotyped FHC cases [3]. The β-MyHC isoform is expressed in ventricular myocardium and in slow-twitch skeletal muscle fibers [4–6]. We have previously studied functional effects of different β-MyHC-missense mutations in slow-twitch fibers of *Musculus soleus*. Data on functional effects of FHC-related β-MyHC-mutations in human ventricular cardiomyocytes are, however, scarce [7–10].

* Corresponding author at: Institute of Molecular and Cell Physiology, Hannover Medical School, Carl Neuberg Str. 1, D-30625 Hannover, Germany. Tel.: +49 511 532 2734; fax: +49 511 532 4296.
E-mail addresses: Kraft.Theresia@mh-hannover.de (T. Kraft), e.paalberends@vumc.nl (E.R. Witjas-Paalberends), n.boontje@vumc.nl (N.M. Boontje), snig_trip@yahoo.com (S. Tripathi), Brandis.Almuth@mh-hannover.de (A. Brandis), Montag.Judith@mh-hannover.de (J. Montag), Hodgkinson.Julie@mh-hannover.de (J.L. Hodgkinson), Francino@clinic.ub.es (A. Francino), 7385fnl@comb.cat (F. Navarro-Lopez), Brenner.Bernhard@mh-hannover.de (B. Brenner), g.stienen@vumc.nl (G.J.M. Stienen), j.vandervelden@vumc.nl (J. van der Velden).

0022-2828
http://dx.doi.org/10.1016/j.yjmcc.2013.01.001

A unique opportunity arose for a direct comparison of effects on myocardium vs. slow twitch skeletal muscle when two severely affected FHC patients carrying β-MyHC-mutation R723G ($MyHC_{723}$) [11] underwent heart transplantation and their LV myocardium became available. The LV of both FHC-patients with $MyHC_{723}$ was functionally equivalent to that of end-stage heart failure (HF). We had previously characterized the $MyHC_{723}$ effects in *M. soleus* fibers from one of these patients [12,13]. Analysis showed that the direct functional effect of the mutation, which is located in the converter domain of the myosin head, is to cause reduced calcium-sensitivity in *soleus* fibers and a 20% increase in maximum force generation. The force increase was found to be due to increased force generation by the individual mutated myosin heads because of increased molecular stiffness. There was no evidence of adaptational processes in the *M. soleus* fibers with $MyHC_{723}$.

Having now both *soleus* and myocardial tissue, in one case even from the same individual, we asked whether the effects of mutation $MyHC_{723}$ on contractile function are the same in cardiomyocytes and slow fibers of *M. soleus*. In addition, this required us to clarify also whether cardiomyocyte function is affected by other alterations of myocardial contractility such as changes in protein phosphorylation. From studies on human cardiac tissue it is known that end-stage HF is characterized by desensitization of the β-adrenergic pathway resulting in e.g., dephosphorylation of cardiac troponin I (cTnI) [14], Myosin-Binding-Protein C (cMyBP-C) [15], and titin [16]. To assess morphological features which might affect function such as myocyte and myofibrillar organization, we also performed structural studies by light- and electron microscopy of ventricular tissue from patients and donors.

2. Methods and materials

An expanded Materials and methods section is included in the online supplementary data.

2.1. Patients and cardiac biopsies

Myocardial tissue was obtained upon cardiac transplant from the LV of a male patient (H27), age 55 years, from family 26, II-5, and a female patient (H29), age 53 years, from family 11, III-8, see Enjuto et al. [11]. Genotyping and clinical details of the patients were published previously [11,17], information about their medication and clinical status at the time of heart transplant are given in Supplementary Table 1. *M. soleus* tissue was obtained from patient H27 one year before HT [12]. Both patients are heterozygous for β-MyHC-mutation R723G and had initially developed the classical clinical phenotype of FHC with diastolic dysfunction, hypertrophy of the LV wall and interventricular septum, ST–T wave abnormalities, pathological Q-wave (patient H29) and heart blocks, similar to other related and unrelated carriers with mutation R723G. The patient's hypertrophic cardiomyopathy eventually progressed into LV dilatation and end-stage systolic heart failure (NYHA III–IV) [11,17]. Development of heart failure is found in a subgroup of FHC patients [2].

Control tissue was from non-transplanted donor hearts ($n = 5$, 23–52 years of age, mean age 39 ± 6 years; 2 female, 3 male) for which no suitable recipient was found. Our previous studies showed no age-dependent differences in any of the parameters of sarcomere function in control cardiomyocytes [18]. For preservation of the tissue see [12] and data supplement. Approval of the local ethics committees and written informed consent for use of the tissue were obtained.

2.2. Force and rate constant of force redevelopment (k_{tr}) measurements in single cardiomyocytes

Force measurements were performed on single, mechanically isolated cardiomyocytes as described previously [19]. Permeabilized single myocytes were attached to a motor and force transducer with silicone adhesive. Force–pCa-relations were obtained from force measurements in solutions of different calcium-concentrations. Maximum active force (F_{max}) was obtained by subtracting passive force from the total force, i.e. $F_{max} = F_{total} - F_{passive}$. k_{tr}, the rate constant of force redevelopment, was measured during isometric contraction after a short period of unloaded isotonic shortening of the myocytes [20]. Force measurements were repeated after incubation of cells with protein kinase A (PKA) or with protein phosphatase-1 (PP-1), i.e. after adjusting phosphorylation levels between donor and $MyHC_{723}$ cardiomyocytes.

2.3. β-Myosin-mRNA quantification

Relative abundance of mutated vs. wild-type *MYH7*-mRNA was determined by a specific restriction digest approach and by real-time PCR (RT-qPCR) as described recently [21]. A detailed description is implemented in the Supplementary material.

2.4. Myofilament protein phosphorylation

Protein phosphorylation was determined as previously described [22]. Tissue samples were separated on gradient gels (Criterion Tris–HCl 4–15% gel, BioRad) and phosphorylated proteins were detected with Pro-Q Diamond staining (Life Technologies, Darmstadt, Germany). For protein content, gels were stained with SYPRO-Ruby (Life Technologies, Darmstadt, Germany). Phosphorylation of myofilament proteins was determined relative to protein expression of cMyBP-C. For two-dimensional gel electrophoresis samples were loaded on immobiline strips with a pH gradient of 4.5 to 5.5 (GE Healthcare, Uppsala, Sweden). In the second dimension, proteins were separated by SDS-PAGE and stained with Coomassie blue. Myosin heavy chain isoform analysis was performed on SDS polyacrylamide gels with 5% polyacrylamide in stacking gel and 8.8% polyacrylamide and 5% glycerol in separation gel. Proteins were separated for 30 h at 4 °C.

2.5. Light- and electron microscopy

Tissue was prepared for histological and electron microscopical (EM) analysis as described [23]. For histology, tissue sections were Elastica van Gieson-stained. Myofibrillar density was analyzed on EM images by calculating the sum of myofibrillar areas over the total cell area in five representative myocytes per sample (total of at least 35 cells).

2.6. Data analysis

Force–pCa relations were fit to a modified Hill-equation [19]. Results are given as mean ± SEM. Differences between donor and $MyHC_{723}$-myocyte groups were examined by two-sample unpaired Student *t*-test with p values < 0.05 considered as statistically significant. Effects of PKA in donor and $MyHC_{723}$ samples, respectively, were tested by one-way ANOVA and Tukey's mean value comparison. A probability value < 0.05 was considered significant for ANOVA.

3. Results

3.1. Unexpected low force generation and unchanged calcium-sensitivity in $MyHC_{723}$ cardiomyocytes

For functional characterization of FHC mutation R723G in cardiac tissue, we investigated isometric force and calcium-sensitivity of isolated, skinned cardiomyocytes (Figs. 1A and B). Cardiomyocytes were isolated from 3 LV wall regions and the septum of patient H27, from one LV region of patient H29, and 5 donors, respectively. Maximum force (F_{max}) was significantly reduced in $MyHC_{723}$ myocytes (23.8 ±

1.7 kN/m^2, 67 cells) compared with donor (34.7 ± 3.8 kN/m^2, 19 cells) (Fig. 1C). Calcium-sensitivity of MyHC$_{723}$ cardiomyocytes (pCa$_{50}$ = 5.56 ± 0.01) was not different from donor cells (pCa$_{50}$ = 5.56 ± 0.01) (Fig. 1D). Both results are strikingly different from data observed previously in slow *M. soleus* fibers of two FHC patients expressing MyHC$_{723}$, one of whom was patient H27. In slow *soleus* fibers with MyHC$_{723}$ F$_{max}$ was increased by 22.8% and the calcium-sensitivity was reduced (ΔpCa$_{50}$ of control vs. MyHC$_{723}$ was 0.14) [12,13]. Comparison of absolute forces at different calcium-concentrations (pCa) in cardiomyocytes from the MyHC$_{723}$ patients (H27 and H29) vs. donor (Fig. 1E), and of *M. soleus* fibers of patient H27 vs. healthy controls (Fig. 1F) reveals the discrepancies in maximum force and calcium dependence of force in the two tissues. The variance of the force–pCa curves in Figs. 1E and F is relatively large because the values are absolute force values of the individual muscle fibers/myocytes which are quite variable mostly due to uncertainties in determination of the cross-sectional area of the cardiomyocytes/fibers. When force–pCa relations are normalized to forces at saturating calcium-concentration (e.g., Fig. 1D), the variance is much smaller, and the shift in the force–pCa-relationship by the MyHC$_{723}$-mutation in *M. soleus* fibers is more obvious (cf. Fig. 5B in [12]).

3.2. Equally high expression level of mutant β-MyHC at mRNA and protein level in both ventricular myocardium and M. soleus

The different effects of MyHC$_{723}$ in cardiomyocytes and *M. soleus* could be due to different levels of MyHC$_{723}$ expression in the FHC myocardium compared to *soleus* fibers. Using both a restriction digest

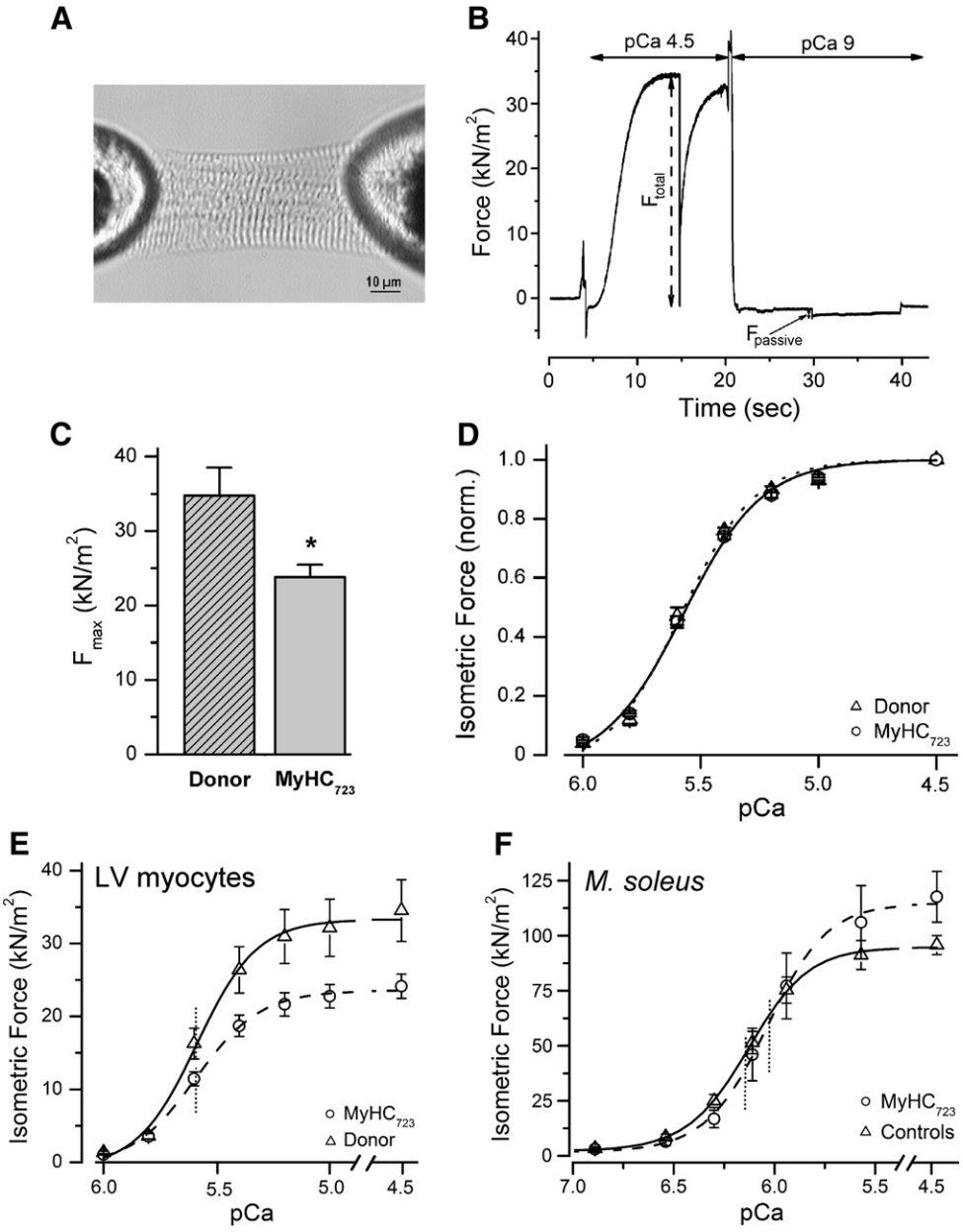

Fig. 1. Force measurements. (A) Cardiomyocyte from the septum of one of the MyHC$_{723}$-patients mounted between motor for length control (left) and force transducer (right). (B) Original force record of single MyHC$_{723}$-myocyte. (C) Maximum active force per cross sectional area at saturating calcium-concentration (F$_{max}$ = F$_{total}$ − F$_{passive}$). F$_{max}$ of MyHC$_{723}$ cardiomyocytes (open bar) is 35% lower than for donor cells (hatched bar; *P<0.05). (D) Force at different calcium concentrations normalized to maximum force at pCa 4.5. Solid and dotted lines, fits of a modified Hill equation yielding pCa$_{50}$. (E) Absolute forces vs. pCa of cardiomyocytes from donor (19 myocytes) and MyHC$_{723}$-patients (66 myocytes). (F) Absolute forces vs. pCa of *M. soleus* fibers of healthy controls and of MyHC$_{723}$-patient H27 (21 fibers, respectively). Dotted vertical lines in (E) and (F) indicate respective pCa$_{50}$ values.

analysis and real-time PCR as recently described [21], the relative abundance of mutated vs. wild-type β-MyHC-mRNA was quantified. In cardiac tissue with $MyHC_{723}$ the fraction of mutated β-MyHC-mRNA was on average 69% for patient H27 in different regions of the LV wall and 67% for patient H29 (Supplementary Table 2). In *M. soleus* of patient H27 and two other patients we previously found a fraction of 66 ± 7% mutated β-MyHC-mRNA. At the protein level, the fraction of mutated β-myosin incorporated into the sarcomeres of *soleus* fibers was 62 ± 6% for patient H27 and his brother [6]. In myocardium, preliminary protein quantification yielded very similar 63 ± 11% of mutated protein [21]. Thus, the extent of expression/incorporation of mutant myosin in the contractile apparatus does not explain the discrepant functional effects between *M. soleus* and myocardium.

3.3. Myocardium-specific reduction in phosphorylation of sarcomeric proteins, which could account for functional differences compared to M. soleus

To test for possible modifiers of contractile properties in myocardium [18,19,24], the phosphorylation status of sarcomeric proteins was determined. Proteins were separated by 1-dimensional gel electrophoresis and stained with phospho-specific stain ProQ Diamond (Fig. 2A) and protein stain SYPRO Ruby (Fig. 2B). Phosphorylation of cMyBP-C, cTnI and myosin light chain 2 (MLC-2) was significantly reduced ($P<0.001$) in $MyHC_{723}$ compared to donor myocardium (Fig. 2C). On average, cMyBP-C and MLC-2 phosphorylation were both reduced to 42% and cTnI phosphorylation to 11% in $MyHC_{723}$ tissue compared to donor tissue. Phosphorylation of cardiac troponin T (cTnT) was significantly reduced only in LV tissue from $MyHC_{723}$ patient H29. The substantial dephosphorylation of cTnI in $MyHC_{723}$ myocardium was confirmed by Western immunoblot using an antibody specific for non-phosphorylated cTnI-PKA sites (serines 23 and 24). The ratio of dephosphorylated cTnI relative to Ponceau-stained actin in $MyHC_{723}$ myocardium was on average 1.66 ± 0.3 (n = 3 samples), while in donor tissue no dephosphorylated cTnI was detected.

Isoform composition and phosphorylation status of ventricular myosin light chains and cTnT in the myocardial samples were assessed using 2D-PAGE [22]. In LV-myocardium of $MyHC_{723}$ both MLC-2 isoforms (MLC-2 and MLC-2*) are dephosphorylated (Fig. 3B) compared to donor tissue (Fig. 3A). However, only the decrease of the phosphorylated MLC-2P and the increase of the unphosphorylated MLC-2* were significant (Table 1). The percentage of phosphorylated MLC-1 did not differ between donor and $MyHC_{723}$ myocardium. On average, cTnT phosphorylation was reduced by 15% in $MyHC_{723}$ tissue compared to donor, while ProQ stained 1D-gels revealed a somewhat larger reduction in cTnT-P of 34%. This is only seen in tissue from patient H29 (Fig. 2C), while for patient H27 cTnT phosphorylation was well preserved (Fig. 3B).

An additional difference between $MyHC_{723}$ and donor ventricular tissue was found for pro-apolipoprotein A-1 (GenBank number AAA51747.1). Pro-apolipoprotein A-1 is a precursor of apolipoprotein A-1, which is involved in lipid transport and metabolism and is a major protein of

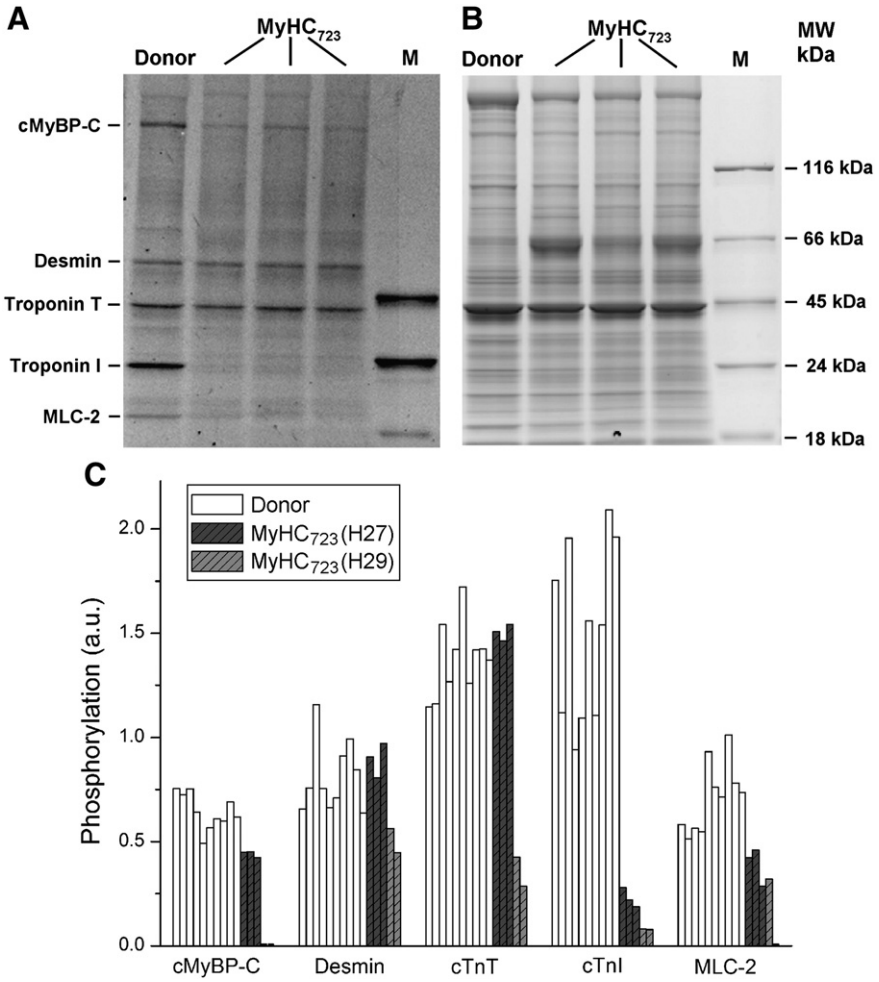

Fig. 2. Phosphorylation status of sarcomeric proteins. (A) ProQ Diamond and (B) SYPRO Ruby stained gels of LV tissue of donor (lane 1) and $MyHC_{723}$-patient H27 (lanes 2–4). Lane 5, marker. (C) Data from donor samples (n = 10 individuals) and samples of two and three different areas of the LV-wall of $MyHC_{723}$-patients H27 and H29, respectively. On average, phosphorylation of cMyBP-C, cTnI and myosin light chain 2 (MLC-2) was significantly reduced in $MyHC_{723}$ compared to donor ($P<0.001$). cTnT-phosphorylation was significantly lower compared to donor tissue only in LV tissue from patient H29.

plasma HDL (high density lipoprotein). Gel-analysis of different parts of the LV of H27 (Fig. 3B) revealed more than five times higher pro-apolipoprotein in septum (pro-apo/actin ratio = 34.6) compared to tissue of two different regions of the free LV wall (pro-apo/actin ratio = 6.3 ± 3) and to donor tissue (Pro-Apo/actin ratio = 2.7).

To see whether MyHC isoform composition contributes to the different mutation effects in cardiomyocytes and slow *M. soleus* fibers, we analyzed the isoforms in the $MyHC_{723}$ ventricular samples using 1D-gel electrophoresis. No significant amounts of α-MyHC could be detected in the samples of the patients (Supplementary Fig. S1). Thus, it is unlikely that isoform composition is responsible for the observed functional differences.

3.4. Reduced calcium-sensitivity in $MyHC_{723}$ myocytes after phosphorylation with PKA

We next examined the influence of the significantly reduced (PKA-dependent) phosphorylation of cTnI and cMyBP-C in $MyHC_{723}$ myocardium on calcium-sensitivity. As described above, the calcium-sensitivity in $MyHC_{723}$ cardiomyocytes did not differ from donor myocytes. When we, however, repeated measurements of force–pCa relations after PKA-treatment to match phosphorylation levels, the resulting reduction in pCa_{50} was much larger in $MyHC_{723}$ ($\Delta pCa_{50} = 0.16 \pm 0.01$, n = 50 cells) than in donor cardiomyocytes ($\Delta pCa_{50} = 0.04 \pm 0.01$, n = 9 cells; $P<0.001$, Table 2). Thus, PKA treatment of donor and $MyHC_{723}$ cardiomyocytes uncovered a significant difference in the force–pCa relationships between $MyHC_{723}$ ($pCa_{50} = 5.40 \pm 0.01$) and donor ($pCa_{50} = 5.51 \pm 0.02$) cells once phosphorylation was maximized for both tissues (Figs. 4A, B). The steepness of the force–pCa relation (Hill coefficient, nH) was very similar for donor and $MyHC_{723}$ cardiomyocytes and not significantly affected by PKA-treatment (Table 2). The reduced calcium-sensitivity in $MyHC_{723}$-cardiomyocytes upon PKA-treatment compared to donor is comparable to the reduced calcium-sensitivity in *M. soleus* fibers with $MyHC_{723}$ (0.14 pCa units) [12].

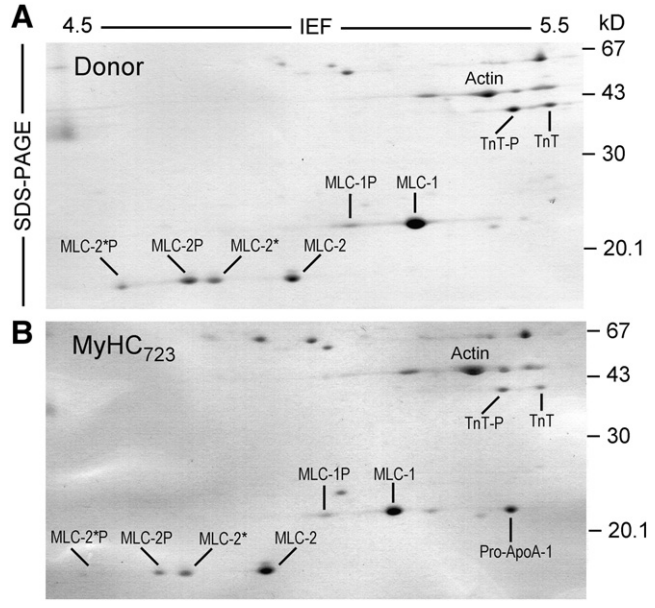

Fig. 3. 2D-gels illustrating MLC composition of donor LV tissue (A) and septum of failing $MyHC_{723}$ myocardium (patient H27; B). IEF, isoelectric focusing; TnT and TnT-P, unphosphorylated and monophosphorylated cardiac troponin T; MLC-1, ventricular myosin light chain 1; MLC-2 and MLC-2*, two isoforms of ventricular myosin light chain 2, both partly phosphorylated (MLC-2P and MLC-2*P, respectively). In septum of $MyHC_{723}$-patient H27 a quite prominent spot is seen, identified by mass spectrometry as pro-apolipoprotein A-1 (Pro-ApoA-1).

Table 1
Abundance of phosphorylated and unphosphorylated ventricular myosin light chains (MLC) 1 and 2 and cardiac troponin T (cTnT) obtained from 2D-IEF-gels.

	Donor	$MyHC_{723}$
cTnT-P	67.0 ± 3.4 (4)	57.1 ± 7.4 (4)
MLC-1P	13.2 ± 2.7 (4)	12.6 ± 1.7 (3)
MLC-2	36.4 ± 4.5 (4)	52.2 ± 6.4 (4)
MLC-2*	20.8 ± 1.6 (4)	27.9 ± 2.5 (4)[a]
MLC-2P	31.9 ± 3.4 (4)	14.7 ± 3.9 (4)[b]
MLC-2*P	11.0 ± 2.2 (4)	5.1 ± 2.9 (4)

Data ± SEM, values in brackets indicate number of tissue samples (donor: n = 4 individuals; $MyHC_{723}$: 2 individuals (H27 and H29), samples from different LV areas (n); cf. Supplementary Table 2). All values are given as percentage of total abundance of the respective protein. MLC-2 and MLC-2*, unphosphorylated MLC-2 isoforms; MLC-2P and MLC2*P, phosphorylated forms. [a]$P = 0.05$ and [b]$P<0.05$, donor vs. $MyHC_{723}$ (*t*-test).

To find out whether the reduced calcium-sensitivity is due to changes in cross-bridge cycling kinetics we recorded the rate constant of force redevelopment (k_{tr}) after PKA-treatment. Fig. 4E shows that k_{tr} at different calcium-concentrations is essentially the same for donor and $MyHC_{723}$ myocytes. For *M. soleus* fibers of controls and $MyHC_{723}$ also no difference in the k_{tr}–pCa relationship was found (data not shown). Nevertheless, the mutation could still cause changes in parameters of cross-bridge cycling kinetics (f_{app} and g_{app}) which do not significantly affect the overall rate constant k_{tr} (see discussion for details).

To test whether the reduced MLC-2 phosphorylation in $MyHC_{723}$ cardiomyocytes might also affect their calcium-sensitivity, we incubated $MyHC_{723}$ and donor cardiomyocytes with protein phosphatase PP-1 [24] and subsequently measured force–pCa relations before and after additional PKA-treatment. PP-1 adjusts all myocytes to a similarly low phosphorylation level particularly of MLC-2 [22,24]. No significant difference of pCa_{50} was observed after treatment with PP-1 (Fig. 4F). Subsequent PKA incubation reduced pCa_{50} to a similar extent as seen without PP-1-pretreatment (Fig. 4A). Phospho-gel analysis of tissue samples after PP-1 and subsequent PKA treatment on average showed similar phosphorylation levels of cMyBP-C, cTnI and MLC-2 for donor and $MyHC_{723}$ hearts (Supplementary Fig. S2). This indicates that the significant reduction of pCa_{50} seen in $MyHC_{723}$ myocytes compared to donor after PP-1–PKA treatment (Fig. 4F) most likely is not due to different phosphorylation levels of these proteins in donor and $MyHC_{723}$ cardiomyocytes. In studies on *M. soleus* fibers, which also showed reduced pCa_{50} with $MyHC_{723}$, all fibers were pre-treated with PP-1 to exclude effects of different phosphorylation of slow MLC-2 (for details see [12]).

3.5. Lower active and passive forces related to structural deficiencies

The lower F_{max} of $MyHC_{723}$ myocytes compared to donor myocytes was not restored by phosphorylation of PKA sites and dephosphorylation of PP-1 sites (Fig. 4D). As a possible reason for the reduction in F_{max}, we looked at changes in morphology of the ventricular tissue at the cellular and subcellular level. Light microscopy (Fig. 5A) of myocardial tissue of both $MyHC_{723}$ patients demonstrated extensive areas with intercellular connective tissue, which was similar in the LV wall of both patients. In the septum of patient H27, it was even more pronounced. This was not seen in donor myocardium. Probably most relevant for the reduced force generation of individual cardiomyocytes are massive changes in sarcomeric ultrastructure of $MyHC_{723}$ compared to donor cardiomyocytes. Electron microscopy revealed not only Z-disc irregularities but also pronounced disarray (Fig. 5B) and reduction in density of myofibrils by 26% in $MyHC_{723}$ cardiomyocytes compared to donor (Fig. 5C). Importantly, in $MyHC_{723}$ cardiomyocytes the observed disarray, i.e., the deviation of the myofibril orientation from a common axis (double arrows in Fig. 5B, bottom panel) indicates a deviation from a common force vector.

Table 2
Calcium-sensitivity (pCa_{50}), Hill coefficient (nH) of force–pCa-relations, active (F_{max}) and passive force ($F_{passive}$), and rate constant of force redevelopment (k_{tr}) at pCa 4.5 of donor vs. $MyHC_{723}$ myocytes before and after treatment with PKA.

	pCa_{50}	nH	F_{max} (kN/m^2)	$F_{passive}$ (kN/m^2)	k_{tr} (1/s)
Donor	5.56 ± 0.01 (19)	3.31 ± 0.21 (19)	34.7 ± 3.8 (19)	4.49 ± 0.59 (19)	0.85 ± 0.05 (19)
$MyHC_{723}$ (H27 & H29)	5.56 ± 0.01 (66)	3.03 ± 0.08 (66)	23.8 ± 1.7[b] (67)	3.24 ± 0.27[b] (67)	0.79 ± 0.03 (64)
After PKA					
Donor	5.51 ± 0.02[a] (9)	3.46 ± 0.23 (8)	33.3 ± 6.5 (8)	4.17 ± 0.88 (8)	0.80 ± 0.07 (8)
$MyHC_{723}$ (H27 & H29)	5.40 ± 0.01[a,b] (50)	3.22 ± 0.09 (50)	24.2 ± 1.8 (51)	2.36 ± 0.23[a,b] (51)	0.81 ± 0.03 (45)

Data ± SEM, number in brackets indicates myocytes measured. Donor includes 5 and 4 individuals before and after PKA, respectively. $MyHC_{723}$ includes two individuals; from patient H27 myocytes from 4 muscle pieces of different LV regions were measured (cf. Supplementary Table 2).
[a] $P<0.05$, before vs. after PKA (one-way ANOVA).
[b] $P<0.05$, donor vs. $MyHC_{723}$ (*t*-test).

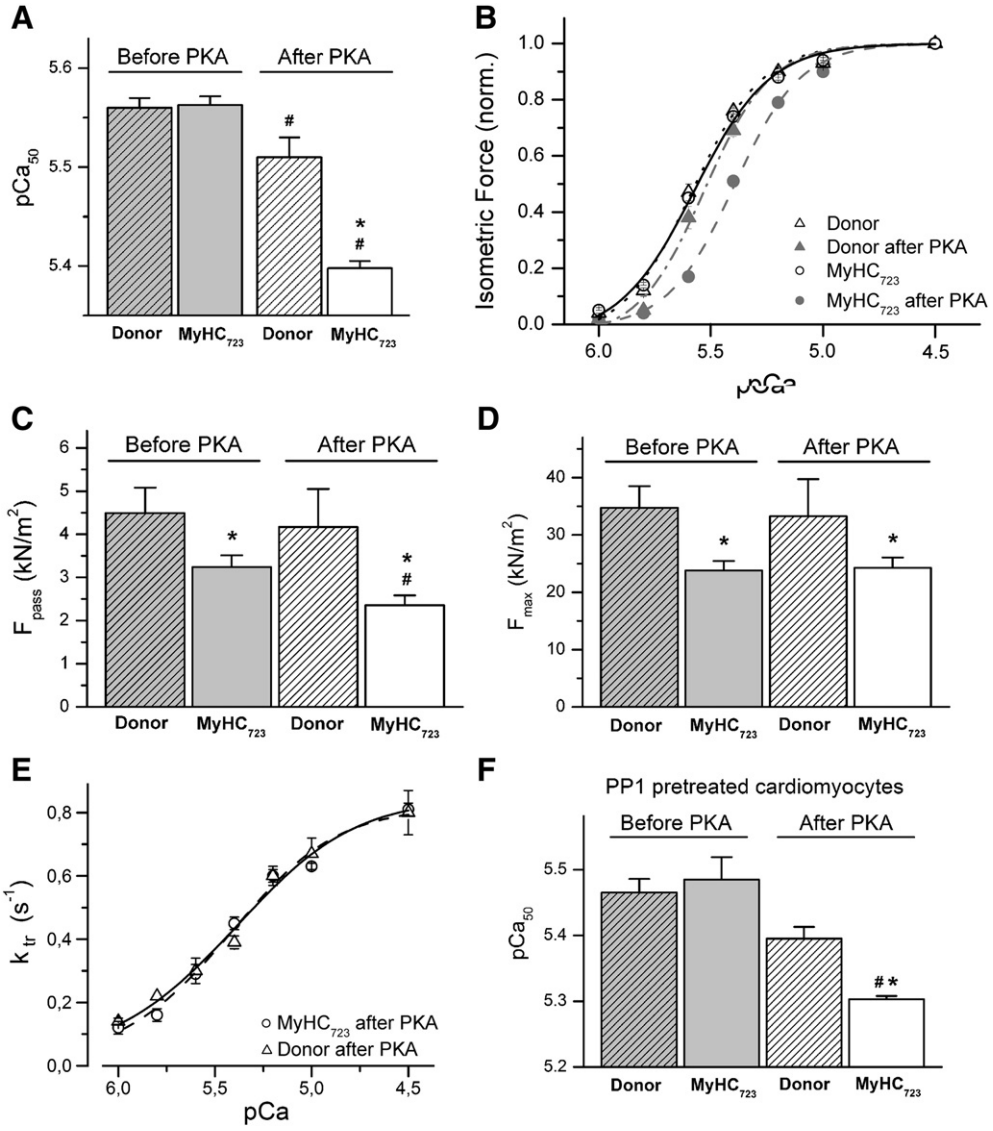

Fig. 4. Effects of PKA-incubation. (A) The calcium-sensitivity (pCa_{50}) is significantly more reduced in $MyHC_{723}$ cells compared to donor cells ($P<0.001$ for ΔpCa_{50}). (B) Force–pCa relations of donor (triangles) and $MyHC_{723}$ cardiomyocytes (circles) before PKA (black open symbols) and after PKA (gray filled symbols) illustrate shift of the $MyHC_{723}$ force–pCa curve to lower calcium-sensitivity after PKA treatment. Modified Hill equation fitted to data points. (C) In untreated cardiomyocytes $F_{passive}$ in $MyHC_{723}$ cardiomyocytes is significantly smaller than in donor. In $MyHC_{723}$ PKA incubation reduced $F_{passive}$ significantly ($P<0.05$). (D) F_{max} in donor and failing $MyHC_{723}$ cardiomyocytes is unaffected by PKA incubation. (E) Rate constant of force redevelopment (k_{tr}) at different calcium-concentrations was essentially the same for donor (triangles) and $MyHC_{723}$ cardiomyocytes (circles). (F) After PP-1-pretreatment, PKA incubation reduced pCa_{50} of $MyHC_{723}$ myocytes significantly ($^{\#}P<0.01$) but non-significantly in donor cells. $^{*}P<0.05$, MyHC723 vs. donor; $^{\#}P<0.05$, before vs. after PKA in A, C and E.

In addition, changes in cross-bridge turnover kinetics could contribute to reduced F_{max} in $MyHC_{723}$ even though the rate constant of force redevelopment (k_{tr}) at saturating calcium concentrations, k_{trmax}, was very similar in $MyHC_{723}$ and donor cardiomyocytes and remained unchanged by PKA-treatment in both groups (Table 2; Fig. 4E). Changes in cross-bridge kinetics, which do not affect k_{tr} could still contribute

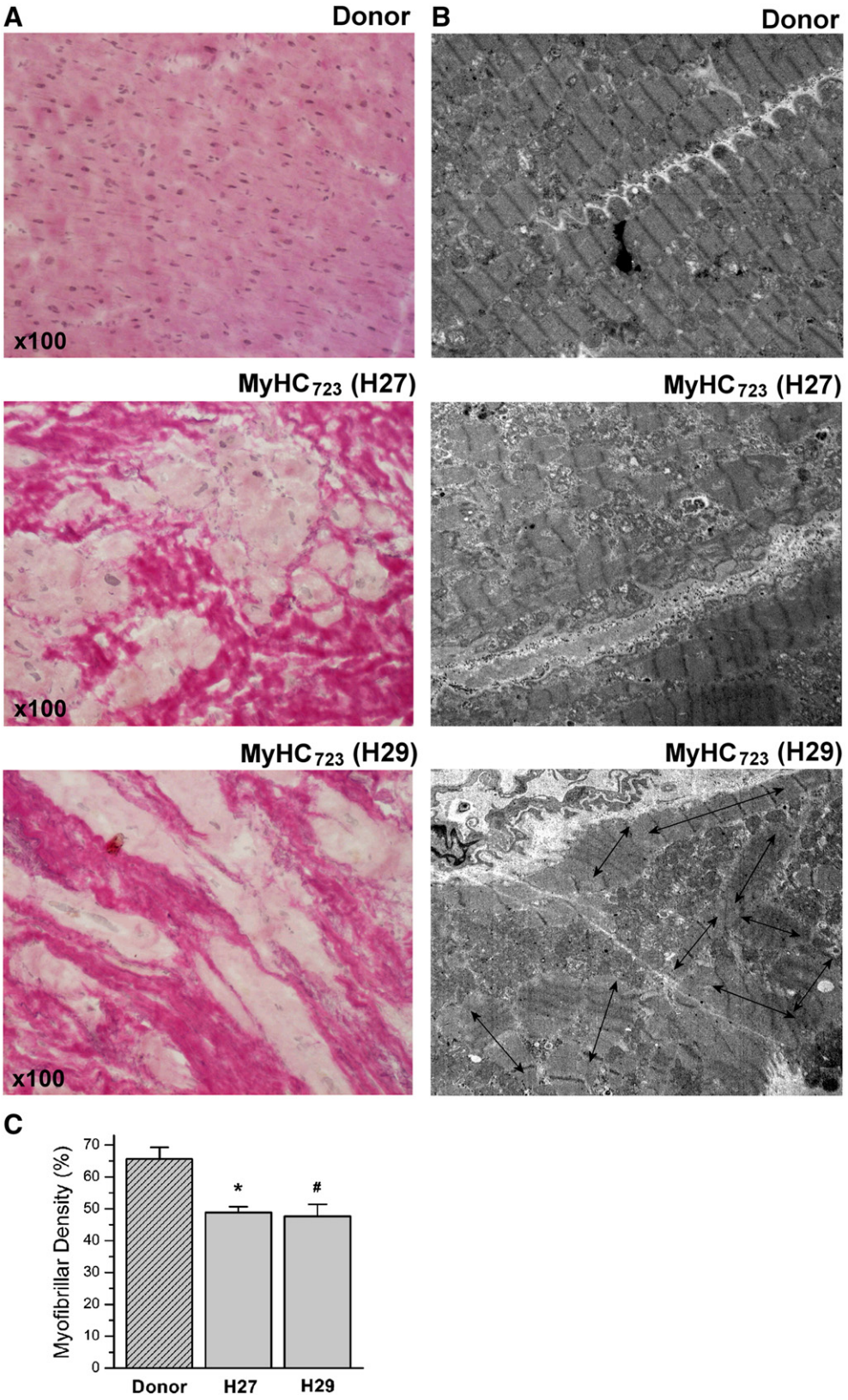

Fig. 5. Light- and electron-microscopy of myocardial tissue and myocyte ultrastructure. (A) Different from donor myocardium, LV myocardium of patients H27 and H29 shows large areas with interstitial connective tissue (dark red in Elastica van Gieson-stained sections; magnification: 100×). (B) At the subcellular level, LV myocardium from donor has well ordered myofibrils and sarcomeres, while in both patients (H27 and H29) Z-discs are irregular, myofibrillar axes are highly variable (disarray, indicated by double arrows) and myofibrillar density is reduced (magnification: 4400×). (C) Substantially reduced myofibrillar density in myocytes of both patients ($^{\#}P<0.01$, $^{*}P<0.001$).

to the reduced force generation of the $MyHC_{723}$ cardiomyocytes (see Discussion for more details).

Besides reduced F_{max}, also $F_{passive}$ was lower in $MyHC_{723}$ cardiomyocytes compared to donor. The difference was 1.25 kN/m^2 (Fig. 4C; Table 2) and increased upon PKA incubation to 1.81 kN/m^2, mainly due to a decrease in $F_{passive}$ for the $MyHC_{723}$ cardiomyocytes. Force at maximum calcium activation (pCa 4.5) was essentially unaffected by PKA-treatment both in $MyHC_{723}$ and donor, i.e. the difference in F_{max} remained unchanged (Fig. 4D; Table 2).

4. Discussion

Changes in contractile function of myocardium triggered by FHC-mutations can be direct effects of such mutations on sarcomeric functions, effects of additional changes like modified protein phosphorylation, or the result of morphological alterations. In the present study, we attempted to discern contributions of these different factors on contractile function of cardiomyocytes with myosin mutation R723G. We (i) analyzed contractile function of $MyHC_{723}$-cardiomyocytes before and after matching protein phosphorylation of donor and $MyHC_{723}$-cardiomyocytes and (ii) analyzed myofibrillar density and organization via EM. Finally, we compared data of $MyHC_{723}$-cardiomyocytes and previous data from *M. soleus* fibers with the same mutation [12].

4.1. Reduced calcium-sensitivity becomes detectable by PKA-treatment

Unexpectedly, the $MyHC_{723}$ cardiomyocytes isolated from tissue samples of affected patients showed the same calcium-sensitivity as donor myocytes. Phosphorylation of cTnI, however, was much lower in both patients' hearts compared to donor myocardium, which is expected to shift the force–pCa relation to higher calcium-sensitivity [19]. Matching phosphorylation levels of donor- and $MyHC_{723}$-cardiomyocytes by phosphorylation of PKA-dependent sites and dephosphorylation of PP-1 sites resulted in reduced calcium-sensitivity of $MyHC_{723}$-cardiomyocytes, which was comparable to the reduced calcium-sensitivity found earlier in *M. soleus* fibers with the same R723G mutation [12]. Such lower calcium-sensitivity is at odds with the idea that FHC-mutations are associated with increased calcium-sensitivity, while in DCM reduced calcium-sensitivity predominates [25,26]. The reason for reduced cTnI-phosphorylation in $MyHC_{723}$-cardiomyocytes is not clear. It could be due to the end-stage HF of the patients since earlier studies on idiopathic dilated and ischemic failing myocardium without sarcomeric mutations showed similarly reduced cTnI-phosphorylation [15,18,19]. The reduced cTnI-phosphorylation, however, might also reflect a hypertrophic cardiomyopathy-typical posttranslational modification as it was also observed in non-failing myectomy-tissue from patients with hypertrophic obstructive cardiomyopathy [9,27].

The reduction in calcium-sensitivity when phosphorylation levels are matched is most likely caused by changes in cross-bridge cycling kinetics. It has been shown that calcium-sensitivity depends on the ratio of the rate constants of cross-bridge cycling, f_{app}/g_{app}. This ratio can modulate contractile function independent of the regulatory protein complex on actin [28]. Isometric force (F) is determined by $F = n \cdot F^* \cdot f_{app}/(f_{app}+g_{app})$ [28], i.e. by the transition of the cross-bridges into force-generating states (f_{app}) and their return to non-force-generating states (g_{app}), by F^*, the mean force generated by each myosin head, and by *n*, the total number of actively cycling myosin heads which can bind to actin within a half sarcomere (depending e.g., on filament overlap). Possible changes in F^* (as found for $MyHC_{723}$ myosin heads [13]) and *n* are expected to affect force generation at each calcium-concentration similarly, therefore changes in these parameters cancel out in normalized force–pCa relationships. It has been shown that an increase in g_{app} and/or a decrease in f_{app}, i.e., any decrease in f_{app}/g_{app} causes reduced force generation with a shift in the force–pCa relationship to the right, i.e., reduced calcium-sensitivity [28].

Measurements of k_{tr} ($k_{tr} = f_{app} + g_{app}$; [28]) revealed essentially no difference for controls and $MyHC_{723}$-cardiomyocytes at all calcium-concentrations. This, however, does not preclude reciprocal changes in the two rate constants that reduce f_{app}/g_{app} but leave $f_{app} + g_{app}$ essentially unchanged. Such reciprocal changes could cause a suppression of maximum force and a decrease in calcium-sensitivity. We calculated possible changes of f_{app} and g_{app} based on the measured values for k_{tr} and for F_{max} at full and half-maximal activation. As value for g_{app} we took 0.17 s^{-1} from data on heart myofibrils at 15 °C (c.f. [10]; slow k_{REL} corresponds to g_{app}). The reduced normalized force of $MyHC_{723}$ cardiomyocytes seen after PKA treatment at half-maximal activation (Fig. 4B) can be accounted for within experimental error by a ~28% increase in g_{app} and a ~40% decrease in f_{app} compared to donor myocytes. The increased unloaded shortening velocity observed in the *M. soleus* fibers also suggests a faster g_{app} for the $MyHC_{723}$ myosin.

In summary, reduced calcium-sensitivity is most likely the result of changes in cycling kinetics of the $MyHC_{723}$ myosin caused by the mutation. F_{max} is also affected by the force contribution of the individual molecule (F^*) which is enhanced for this mutation due to increased resistance to elastic distortion [13]. Thus, increased force contribution per myosin molecule and reduced calcium-sensitivity are not contradictory.

4.2. Reduced maximum active and passive forces

The reduced F_{max} in $MyHC_{723}$ cardiomyocytes by 31% is in strong contrast to 20% increase in F_{max} of *soleus* fibers with this mutation [13]. For patient H27 the skeletal biopsy was taken only one year before the heart transplant, this short time difference is unlikely to be responsible for such drastic force reduction. Reduced F_{max} is in contrast to most findings in non-FHC-related heart failure where F_{max} is often unchanged [29]. However, in cardiomyocytes isolated from myectomy tissue of hypertrophic cardiomyopathy patients with LV outflow tract obstruction F_{max} was also reduced [9,27]. Similar expression levels of mutated β-MyHC-mRNA and protein in myocardium and *soleus* [21] showed that the discrepancy is not due to altered expression of mutated myosin. In addition, studies using X-ray diffraction and confocal microscopy indicated that myosin-converter-domain mutations like R723G, R719W or G741R, do not alter sarcomeric composition and ordered assembly of myofilaments in triton-permeabilized *M. soleus* fibers ([30], own unpublished observations). In general, assembly and formation of the thick filaments are normal with other myosin head-domain mutations [31].

Most likely, a substantial part of the reduced F_{max} in $MyHC_{723}$ cardiomyocytes is due to the significantly lower density and the disarray of myofibrils observed by electron microscopy. We estimated F_{max} of the $MyHC_{723}$ myocytes expected if myofibrillar density were not lowered by 26%. In this case, F_{max} would be increased from 24.2 kN/m^2 (Table 2) to 32.8 kN/m^2, which is essentially the same as F_{max} of the donor myocytes. Besides lower myofibrillar density electron microscopy also showed that myofibrils in $MyHC_{723}$ cardiomyocytes deviate from the major force axis. Such myofibrils will only partly contribute to maximum force generation in axial direction, as has been shown for similarly compromised microarchitecture in dystrophic muscle cells [32]. Thus, reduced F_{max} caused by disarray and reduced number of myofibrils very likely outweighs the increased force per myosin head caused by the mutation, as seen in *M. soleus* fibers with $MyHC_{723}$ [13]. *M. soleus* fibers of controls and $MyHC_{723}$ patients both have a highly ordered sarcomeric structure and show no indication of reduced myofibrillar density.

Phosphorylation of PKA sites and dephosphorylation of PP-1 sites did not restore F_{max} of $MyHC_{723}$ myocytes. Thus, PKA- and PP-1-dependent signaling does not contribute to the reduced F_{max}. This is supported by previous work on failing myocardium with similarly low MLC-2 phosphorylation showing unaltered F_{max} of cardiomyocytes [19]. However, it cannot be completely excluded that different MLC-isoform expression in *soleus* and myocardium may contribute to different effects of mutation

R723G on F_{max}. In *soleus* only the MLC-2-isoform (slow/ventricular) is present and a different essential light chain (MLC-1slow-a) can be expressed [4]. Yet, the MLC-1 is in very close proximity to the converter region of the myosin head domain where the mutation is located. Therefore, changes in possible interactions between myosin heavy chain and MLC-1 could influence the effect of $MyHC_{723}$ on stiffness and force of the individual mutated myosin heads [13] and thus affect F_{max} differently in *M. soleus* and cardiomyocytes.

$F_{passive}$ of myocytes mainly depends on the elastic properties of titin, which spans each half sarcomere from the Z-disc to the M-line, anchoring the myosin filaments. Therefore, the loss and distortion of myofibrils may also explain the 28% lower $F_{passive}$ of $MyHC_{723}$ cardiomyocytes. This is actually different from heart failure [24] and from cardiomyocytes isolated from myectomy tissue of patients with hypertrophic cardiomyopathy [9,27] where $F_{passive}$ was unchanged. The additional reduction of $F_{passive}$ by rephosphorylation with PKA could well be a direct consequence of titin phosphorylation [33], indicating dephosphorylated titin in the failing FHC myocardium. For the patient's myocardial function and particularly for impaired diastolic filling, however, the massive interstitial fibrosis of the left ventricular wall and of the septum seen in histology is probably the major disadvantage, despite the reduced $F_{passive}$ of the isolated cardiomyocytes.

4.3. The course of FHC development

With a study on cardiac samples from FHC patients at end-stage heart failure it is essentially not possible to assess initial effects and early stages of the development of FHC phenotype features. However, based on functional studies on *M. soleus* fibers with the same mutation [12,13] and on analysis of expression levels of mutated myosin in myocardium and *M. soleus* of the heterozygous patients [21], we may develop the following hypothesis: We assume that the mutation effects observed in *M. soleus* fibers, where no myofibrillar deficiencies and phosphorylation changes were obvious, reflect the situation in cardiomyocytes of the patients at the very beginning of the disease. In this case, in $MyHC_{723}$ cardiomyocytes at early stages of disease only a slight change of average force generation at submaximal calcium-concentrations would be detectable (Fig. 1F) and major adaptations and myofibrillar deficiencies may still be absent.

We hypothesize that subsequently disarray develops in myocardium because of variable expression of mutated and wild-type myosin in individual myocytes, resulting in functional variability among individual cells [12,21]. This is based on studies on $MyHC_{723}$ muscle fibers where we found, different from control fibers, large variability in calcium-sensitivity and force generation among individual $MyHC_{723}$-fibers ranging from near normal values to highly significant deviations from control [12]. If in myocardium similar variability exists among neighboring cardiomyocytes at early stages of the disease, imbalances in force generation among cardiomyocytes and myofibrils will trigger non-uniform contraction of myocardial tissue, i.e., overcontraction vs. overstretching of individual myocytes. Due to the arrangement of cardiomyocytes in a network with cells in series and branched cells, in the long run non-uniform contraction results in cellular and myofibrillar disarray. In *M. soleus*, due to the unbranched, parallel arrangement of fibers, no such disarray is expected to develop. In myocardium, disarray with structural damage or even loss of myocytes under increased strain will cause impaired force output, presumably triggering hypertrophy for compensation. Alterations of contractile function of cardiomyocytes such as reduced cTnI-phosphorylation always affect both mutated and wild-type acto-myosin-complexes in the same way, and therefore cannot compensate for the imbalances in force generation. To test unequal $MyHC_{723}$ expression which is the basis of this hypothesis requires downscaling of β-MyHC-mRNA quantification to the level of individual cardiomyocytes.

In conclusion, the observed functional differences between *M. soleus* fibers and cardiomyocytes with mutation $MyHC_{723}$ can be explained by alterations of protein phosphorylation and morphology of $MyHC_{723}$-cardiomyocytes. These alterations could be due to HF in these patients but might also reflect FHC-phenotype-related posttranslational modifications, as these were observed in myectomy-tissue from patients with hypertrophic obstructive cardiomyopathy without HF [9,27]. Thus, in the case of MyHC-mutations in FHC, *M. soleus* biopsies appear useful for functional studies trying to identify direct effects of FHC-mutations and to suggest strategies for early prevention of FHC-typical features in young mutation carriers. Yet, long-term studies on contractility and ultrastructure of the myocardium of genotyped family members beginning at very young age and studies on animal models with near human physiology are needed to more completely understand human FHC-pathogenesis.

Disclosure statement

None declared.

Acknowledgments

The authors thank Ruud Zaremba (Cardiovascular Research, VU Amsterdam, Netherlands), Birgit Piep and Alexander Lingk (Molecular and Cell Physiology, Hannover Medical School, Germany), and Adelheid Müller-Friedrichsen (Pathology, Hannover Medical School, Germany) for excellent technical support.

Funding sources: This work was supported by grants (KR 1187/5-4 and KR 1187/19-1) of the Deutsche Forschungsgemeinschaft to TK, the Seventh Framework Program of the European Union "BIG-HEART," grant agreement 241577 to JvdV and a VIDI grant from the Netherlands organization for scientific research (NWO) to JvdV.

Appendix A. Supplementary data

Supplementary data to this article can be found online at http://dx.doi.org/10.1016/j.yjmcc.2013.01.001.

References

[1] Maron BJ, Gardin JM, Flack JM, Gidding SS, Kurosaki TT, Bild DE. Prevalence of hypertrophic cardiomyopathy in a general population of young adults. Echocardiographic analysis of 4111 subjects in the CARDIA Study. Coronary Artery Risk Development in (Young) Adults. Circulation 1995;92:785–9.
[2] Maron BJ, McKenna WJ, Danielson GK, Kappenberger LJ, Kuhn HJ, Seidman CE, et al. American College of Cardiology/European Society of Cardiology Clinical Expert Consensus Document on Hypertrophic Cardiomyopathy. A report of the American College of Cardiology Foundation Task Force on Clinical Expert Consensus Documents and the European Society of Cardiology Committee for Practice Guidelines. Eur Heart J 2003;24:1965–91.
[3] Richard P, Charron P, Carrier L, Ledeuil C, Cheav T, Pichereau C, et al. Hypertrophic cardiomyopathy: distribution of disease genes, spectrum of mutations, and implications for a molecular diagnosis strategy. Circulation 2003;107:2227–32.
[4] Schiaffino S, Reggiani C. Molecular diversity of myofibrillar proteins: gene regulation and functional significance. Physiol Rev 1996;76:371–423.
[5] Cuda G, Fananapazir L, Zhu WS, Sellers JR, Epstein ND. Skeletal muscle expression and abnormal function of beta-myosin in hypertrophic cardiomyopathy. J Clin Invest 1993;91:2861–5.
[6] Becker E, Navarro-Lopez F, Francino A, Brenner B, Kraft T. Quantification of mutant versus wild-type myosin in human muscle biopsies using nano-LC/ESI–MS. Anal Chem 2007;79:9531–8.
[7] Cuda G, Fananapazir L, Epstein ND, Sellers JR. The in vitro motility activity of beta-cardiac myosin depends on the nature of the beta-myosin heavy chain gene mutation in hypertrophic cardiomyopathy. J Muscle Res Cell Motil 1997;18:275–83.
[8] Jacques AM, Briceno N, Messer AE, Gallon CE, Jalilzadeh S, Garcia E, et al. The molecular phenotype of human cardiac myosin associated with hypertrophic obstructive cardiomyopathy. Cardiovasc Res 2008;79:481–91.
[9] Hoskins AC, Jacques A, Bardswell SC, McKenna WJ, Tsang V, dos Remedios CG, et al. Normal passive viscoelasticity but abnormal myofibrillar force generation in human hypertrophic cardiomyopathy. J Mol Cell Cardiol 2010;49:737–45.
[10] Belus A, Piroddi N, Scellini B, Tesi C, Amati GD, Girolami F, et al. The familial hypertrophic cardiomyopathy-associated myosin mutation R403Q accelerates tension generation and relaxation of human cardiac myofibrils. J Physiol 2008;586:3639–44.

[11] Enjuto M, Francino A, Navarro-Lopez F, Viles D, Pare JC, Ballesta AM. Malignant hypertrophic cardiomyopathy caused by the Arg723Gly mutation in beta-myosin heavy chain gene. J Mol Cell Cardiol 2000;32:2307–13.
[12] Kirschner SE, Becker E, Antognozzi M, Kubis HP, Francino A, Navarro-Lopez F, et al. Hypertrophic cardiomyopathy-related beta-myosin mutations cause highly variable calcium sensitivity with functional imbalances among individual muscle cells. Am J Physiol Heart Circ Physiol 2005;288:H1242–51.
[13] Seebohm B, Matinmehr F, Köhler J, Francino A, Navarro-Lopez F, Perrot A, et al. Cardiomyopathy mutations reveal variable region of myosin converter as major element of cross-bridge compliance. Biophys J 2009;97:806–24.
[14] Bodor GS, Oakeley AE, Allen PD, Crimmins DL, Ladenson JH, Anderson PA. Troponin I phosphorylation in the normal and failing adult human heart. Circulation 1997;96:1495–500.
[15] El-Armouche A, Pohlmann L, Schlossarek S, Starbatty J, Yeh YH, Nattel S, et al. Decreased phosphorylation levels of cardiac myosin-binding protein-C in human and experimental heart failure. J Mol Cell Cardiol 2007;43:223–9.
[16] Borbely A, Falcao-Pires I, van Heerebeek L, Hamdani N, Edes I, Gavina C, et al. Hypophosphorylation of the Stiff N2B titin isoform raises cardiomyocyte resting tension in failing human myocardium. Circ Res 2009;104:780–6.
[17] Borchert B, Tripathi S, Francino A, Navarro-Lopez F, Kraft T. The left and right ventricle of a patient with a R723G mutation of the beta-myosin heavy chain and severe hypertrophic cardiomyopathy show no differences in the expression of myosin mRNA. Cardiol J 2010;17:518–22.
[18] Hamdani N, Borbely A, Veenstra SP, Kooij V, Vrydag W, Zaremba R, et al. More severe cellular phenotype in human idiopathic dilated cardiomyopathy compared to ischemic heart disease. J Muscle Res Cell Motil 2010;31:289–301.
[19] van der Velden J, Papp Z, Zaremba R, Boontje NM, de Jong JW, Owen VJ, et al. Increased Ca^{2+}-sensitivity of the contractile apparatus in end-stage human heart failure results from altered phosphorylation of contractile proteins. Cardiovasc Res 2003;57:37–47.
[20] Brenner B, Eisenberg E. Rate of force generation in muscle: correlation with actomyosin ATPase activity in solution. Proc Natl Acad Sci U S A 1986;83:3542–6.
[21] Tripathi S, Schultz I, Becker E, Montag J, Borchert B, Francino A, et al. Unequal allelic expression of wild-type and mutated beta-myosin in familial hypertrophic cardiomyopathy. Basic Res Cardiol 2011;106:1041–55.
[22] Zaremba R, Merkus D, Hamdani N, Lamers JM, Paulus WJ, Dos Remedios C, et al. Quantitative analysis of myofilament protein phosphorylation in small cardiac biopsies. Proteomics Clin Appl 2007;1:1285–90.
[23] van Heerebeek L, Borbely A, Niessen HW, Bronzwaer JG, van der Velden J, Stienen GJ, et al. Myocardial structure and function differ in systolic and diastolic heart failure. Circulation 2006;113:1966–73.
[24] van der Velden J, Papp Z, Boontje NM, Zaremba R, de Jong JW, Janssen PM, et al. The effect of myosin light chain 2 dephosphorylation on Ca^{2+}-sensitivity of force is enhanced in failing human hearts. Cardiovasc Res 2003;57:505–14.
[25] Robinson P, Mirza M, Knott A, Abdulrazzak H, Willott R, Marston S, et al. Alterations in thin filament regulation induced by a human cardiac troponin T mutant that causes dilated cardiomyopathy are distinct from those induced by troponin T mutants that cause hypertrophic cardiomyopathy. J Biol Chem 2002;277:40710–6.
[26] Robinson P, Griffiths PJ, Watkins H, Redwood CS. Dilated and hypertrophic cardiomyopathy mutations in troponin and alpha-tropomyosin have opposing effects on the calcium affinity of cardiac thin filaments. Circ Res 2007;101:1266–73.
[27] van Dijk SJ, Paalberends ER, Najafi A, Michels M, Sadayappan S, Carrier L, et al. Contractile dysfunction irrespective of the mutant protein in human hypertrophic cardiomyopathy with normal systolic function. Circ Heart Fail 2012;5:36–46.
[28] Brenner B. Effect of Ca^{2+} on cross-bridge turnover kinetics in skinned single rabbit psoas fibers: implications for regulation of muscle contraction. Proc Natl Acad Sci U S A 1988;85:3265–9.
[29] van der Velden J, Klein LJ, Zaremba R, Boontje NM, Huybregts MA, Stooker W, et al. Effects of calcium, inorganic phosphate, and pH on isometric force in single skinned cardiomyocytes from donor and failing human hearts. Circulation 2001;104:1140–6.
[30] Köhler J, Winkler G, Schulte I, Scholz T, McKenna W, Brenner B, et al. Mutation of the myosin converter domain alters cross-bridge elasticity. Proc Natl Acad Sci U S A 2002;99:3557–62.
[31] Becker KD, Gottshall KR, Hickey R, Perriard JC, Chien KR. Point mutations in human beta cardiac myosin heavy chain have differential effects on sarcomeric structure and assembly: an ATP binding site change disrupts both thick and thin filaments, whereas hypertrophic cardiomyopathy mutations display normal assembly. J Cell Biol 1997;137:131–40.
[32] Friedrich O, Both M, Weber C, Schurmann S, Teichmann MD, von Wegner F, et al. Microarchitecture is severely compromised but motor protein function is preserved in dystrophic mdx skeletal muscle. Biophys J 2010;98:606–16.
[33] Yamasaki R, Wu Y, McNabb M, Greaser M, Labeit S, Granzier H. Protein kinase A phosphorylates titin's cardiac-specific N2B domain and reduces passive tension in rat cardiac myocytes. Circ Res 2002;90:1181–8.